

Quantum geometric formulation of Brans-Dicke theory for Bianchi I spacetime

Manabendra Sharma,^{1,2,*} Gustavo S. Vicente,^{3,†} Leila L. Graef,^{4,‡} Rudnei O. Ramos,^{5,§} and Anzhong Wang^{6,¶}

¹*Centre for Theoretical Physics and Natural Philosophy,*

Nakhonsawan Studiorum for Advanced Studies, Mahidol University, Nakhonsawan 60130, Thailand

²*Inter University Centre for Astronomy and Astrophysics, Post Bag 4, Pune 411007, India*

³*Faculdade de Tecnologia, Universidade do Estado do Rio de Janeiro, 27537-000 Resende, RJ, Brazil*

⁴*Instituto de Física, Universidade Federal Fluminense, 24210-346 Niteroi, RJ, Brazil*

⁵*Departamento de Física Teórica, Universidade do Estado do Rio de Janeiro, 20550-013 Rio de Janeiro, RJ, Brazil*

⁶*GCAP-CASPER, Department of Physics and Astronomy,
Baylor University, Waco, Texas 76798-7316, USA*

(Dated: February 21, 2025)

This paper investigates Bianchi I spacetimes within the Jordan frame of Brans-Dicke theory, incorporating the framework of effective loop quantum gravity. After developing general formulas, we analyze the robustness of classical singularity resolution due to quantum geometric effects using two common quantization schemes. We then compare the resulting physical properties. We find that both schemes replace classical singularities with regular quantum bounces. Notably, in contrast to similar studies based on general relativity, we find that all three directional scale factors of the Bianchi I spacetimes increase and after the quantum bounce they reach values similar to their initial values, leading to a merging with classical spacetimes in both schemes.

I. INTRODUCTION

Loop quantum gravity (LQG) is a candidate of quantum gravity theory, which takes the premise of gravity as a manifestation of geometry of spacetime and systematically constructs a theory of quantum Riemannian geometry with rigor (see, e.g., Ref. [1] for a recent review). LQG stands out as a nonperturbative background independent approach to quantize gravity [2–6]. At its depth, this theory brings out a fundamental discreteness at Planck scale wherein the underlying geometric observables, such as areas of physical surfaces and volumes of physical regions, are discrete in nature [7–10]. At present, the studies in cosmology and black holes provide ones of the major avenues for applying and testing the ideas of the theory. The absence of the possibility to design a table top experiment, other than thought experiment, can be easily understood from the energy scale involved in LQG, which is by far beyond the reach of present technology. However, it is feasible to apply LQG against observational physics in the context of quantum cosmology. In fact, the early Universe provides a natural laboratory for this purpose, and it is very interesting and important to investigate the Planckian physics of the very early Universe in the framework of LQG.

Loop quantum cosmology (LQC) is an application of LQG techniques to the symmetry reduced spacetimes [11–16]. In LQC the big bang singularity is resolved in the sense that it is replaced by a quantum bounce, across which physical observables, such as energy density

and curvatures, which diverge at the big bang singularity in classical general relativity (GR), now all remain finite. This nondivergent behavior owes to the fact that in LQG the area operator has a discrete spectrum of eigenvalues with a nonzero area gap [7–10]. It is this nonzero gap that prevents the formation of spacetime singularities [17–19]. This is quite similar to the simple harmonic oscillator, whose ground state energy is not zero quantum mechanically, although classically it does. Remarkably, LQC produces a contracting Friedmann-Lemaître-Robertson-Walker (FLRW) Universe that bounces back to an expanding one, thus, avoiding the occurrence of a singularity. This is achieved without adding any nontrivial matter component, unlike in the case of classical or matter bounces (see, e.g., Refs. [20–22]). This quantum bounce occurs purely due to quantum geometric effects, a novel repulsive effective force that is manifest in the quantum corrected Friedmann and Raychaudhuri equations. The massless scalar field that acts as a clock in this setting, is identified with the inflaton that drives a nearly exponential expansion of the Universe given by the effective dynamics. The preinflationary background dynamics have been extensively studied in detail for various forms of potentials in the Refs. [23–27]. In addition, in all spacetimes studied so far, which permit different symmetries, including the Bianchi and Gowdy models [28–47], the singularity is resolved [11–16].

An important issue that appears in the bouncing scenario is the possible instability in the growth of anisotropic density during the contracting phase. As a matter of fact, during this contraction phase, the contribution from anisotropic stresses to the Friedmann equation grows much faster than the energy density of the usual fields, like radiation, baryonic matter and cold dark matter. Once the ratio of the anisotropic stresses to the total energy density becomes comparable, it is not possible any longer to assume that the background

* sharma.man@mahidol.ac.th

† gustavo@fat.uerj.br

‡ leilagraef@id.uff.br

§ rudnei@uerj.br

¶ Anzhong.Wang@baylor.edu

spacetime is approximately isotropic, and this ratio can even become larger than unity, eventually leading to an anisotropic collapse. When considering inhomogeneities, the situation is even more sensitive. In particular, when the ratio of the anisotropic stresses to the total energy density is larger than unity, it indicates the onset of the conjectured Belinski-Khalatnikov-Lifshitz chaotic instability [48]. As is well-known, due to the high sensitivity of the dynamics to the initial conditions (neighboring points following very different dynamics), this scenario can lead to the loss of predictivity. In this case, the large anisotropies impact the density fluctuations in a highly inhomogeneous way, spoiling the prediction of a nearly isotropic cosmic microwave background [49, 50]. This can be avoided, for example, in some situations when the nearly scale-invariant perturbations are generated after the bounce [51]. Furthermore, in the special case of the Bianchi type I model [52], it was shown that isotropization is an attractor, which makes this scenario a natural choice to investigate viable candidates. This is especially promising in the framework of LQC, where we can analyze the Bianchi I background in a bouncing scenario driven by modifications to the Einstein equations in the high energy regime. Great efforts have been devoted towards understanding the quantum corrected dynamics of anisotropic spacetime starting with the Einstein-Hilbert action (see, for example, Refs. [28–47] and references therein).

A natural question to ask is what will happen when one goes beyond the Einstein-Hilbert action. One of the salient features of GR is that all the geometrical quantities, such as distance, area and volume can be constructed from the knowledge of the metric. The metric and, hence, the geometry of the spacetime, being a dynamical quantity that is determined by the distribution of matter and energy. These fundamental properties of the theory remain intact even beyond the minimally coupled Einstein-Hilbert action. This motivates us to consider an action with a nonminimal coupling term and to find the corresponding quantum corrected dynamics. As an example toward this goal, we consider the Brans-Dicke theory (BDT). In particular, the techniques of LQG are not limited to a particular action. Based on the loop quantization, some aspects of its implementation in the context of the BDT has been explored for the FLRW spacetime [53–57] and the presence of a quantum bounce is shown in both the Jordan and Einstein frames.

One of the prime focus of the present paper is to formulate the quantum corrected effective dynamics of BDT in homogeneous and anisotropic Bianchi I spacetimes in the Jordan frame, whose study is still missing in the literature, as far as we are aware of. This is a crucial step towards establishing and checking the robustness of the major results of loop quantization in spacetimes with different symmetries and different theories of gravity. In particular, we aim to ultimately check the robustness of the singularity resolution and the consistency of the effective dynamics.

This paper is organized as follows. In Sec. II, we briefly review the Hamiltonian formulation of BDT and provide the necessary formulas for the studies of Bianchi I spacetimes in Jordan’s frame of the theory. In Sec. III, we present the symmetry reduction of the classical Hamiltonian constraint for Bianchi I spacetimes and write down the corresponding classical dynamical equations. In Sec. IV, we study the quantum corrected dynamics using two alternative and complementary quantization schemes, which have been considered in the literature, and write down the dynamical equations for each of the schemes. In order to study quantum effects of matter fields, in the effective Hamiltonian, we also include a massless scalar field Φ , in addition to the Brans-Dicke (BD) scalar field ϕ . In Sec. V, we study numerically the dynamics of the BDT for Bianchi LQC models in both quantization schemes and show explicitly that the classical spacetime singularity is indeed resolved in both schemes and replaced by a quantum bounce. Our main conclusions are presented in Sec. VI. Throughout this work, we will adopt the convention $M_{\text{Pl}} = 1$ (unless in the cases where possible confusions can raise), where $M_{\text{Pl}} \equiv 1/\sqrt{8\pi G}$ is the reduced Planck mass.

II. HAMILTONIAN FORMULATION OF BRANS-DICKE THEORY

To facilitate our investigations to be carried out in the next sections, in this section we shall provide a very brief review of BDT and for more details, we refer the readers to [53–57]. The BDT is described by the action

$$S_{\text{BDT}} = \frac{1}{2} \int d^4x \sqrt{-g} \left(\phi R - \frac{\omega}{\phi} g^{\mu\nu} \partial_\mu \phi \partial_\nu \phi \right), \quad (2.1)$$

where R is the Ricci scalar, $g_{\mu\nu}$ the metric and g its determinant. The BD scalar field is denoted by ϕ and ω is the coupling constant, which is highly constrained observationally [58]. The present format of covariant formulations of the theory is not suitable for loop quantization. In the Lagrangian formulation, space and time are treated on equal footing, but the construction of the canonical formula demands splitting of spacetime into space and time. It is the Arnowitt-Deser-Misner formalism [4, 59, 60] with the 3+1 decomposition that comes to rescue the situation by providing a description in terms of the first-order Hamilton’s equations of the phase space variables. Formally, this can be represented by decomposing the spacetime manifold, \mathcal{M} endowed with a metric, designated by the pair $(\mathcal{M}, g_{\mu\nu})$, into (Σ, \mathbb{R}) , where Σ represents the spatial three-dimensional hypersurface and \mathbb{R} stands for the real valued time.

The splitting of the metric into its intrinsic spatial metric q_{ab} ($a, b = 1, 2, 3$) and the normal vector n_μ ($n_\nu n^\nu = -1$) to the hypersurface naturally introduces the notion of extrinsic curvature, K_{ab} , defined in terms of covariant derivative of the normal vector to the hypersurface as projected to the hypersurface [61]. Let us denote q

as the determinat of q_{ab} and N denotes the lapse function. Then, the corresponding conjugate momenta for the BDT action given by Eq. (2.1) are

$$p^{ab} \equiv \frac{\delta \mathcal{L}}{\delta \dot{q}_{ab}} = \frac{\sqrt{q}}{2} \left[\phi (K^{ab} - K q^{ab}) - \frac{q^{ab}}{N} (\dot{\phi} - N^c \partial_c \phi) \right], \quad (2.2)$$

$$p_\phi \equiv \frac{\delta \mathcal{L}}{\delta \dot{\phi}} = -\sqrt{q} \left[K - \frac{w}{N\phi} (\dot{\phi} - N^c \partial_c \phi) \right], \quad (2.3)$$

$$p_N(x) \equiv \frac{\delta \mathcal{L}}{\delta \dot{N}(x)} = 0, \quad (2.4)$$

$$p_a(x) \equiv \frac{\delta \mathcal{L}}{\delta \dot{N}^a(x)} = 0, \quad (2.5)$$

where the Lagrangian density \mathcal{L} is given by [62]

$$\begin{aligned} \mathcal{L} = & \frac{\sqrt{q}}{2\kappa^2} \left[N\phi (\mathcal{R} + (K^{ab}K_{ab} - K^2)) + 2q^{ab}D_a N D_b \phi \right. \\ & - \frac{w}{N\phi} \left(N^2 q^{ab} D_a \phi D_b \phi - (\dot{\phi} - N^a D_a \phi)^2 \right) \\ & \left. - 2K(\dot{\phi} - N^a D_a \phi) \right]. \end{aligned} \quad (2.6)$$

Here the trace of the extrinsic curvature tensor is $K \equiv K_a^a = q^{ab}K_{ab}$ and the spatial covariant derivative is defined as $D_a \equiv q_a^b \nabla_b$. For a given Lagrangian, the Hamiltonian can be obtained by the Legendre transformation,

$$H_{\text{total}} = \int_{\Sigma} d^3x \sqrt{q} (\dot{q}_{ab} p^{ab} + \dot{\phi} p_\phi - \mathcal{L}(q_{ab}, \dot{q}_{ab})), \quad (2.7)$$

which can be cast in the form

$$\begin{aligned} H_{\text{total}} = & \int_{\Sigma} d^3x N^a \left[-2D^b p_{ab} + p_\phi \partial_a \phi \right] \\ & + \int_{\Sigma} d^3x N \left\{ \frac{2}{\sqrt{q}\phi} \left[p_{ab} p^{ab} - \frac{1}{2} p^2 + \frac{(p - p_\phi \phi)^2}{2(3+2w)} \right] \right. \\ & \left. + \frac{\sqrt{q}}{2} \left[-\phi R + \frac{w}{\phi} (D_a \phi) D^a \phi + 2D_a D^a \phi \right] \right\}, \end{aligned} \quad (2.8)$$

In terms of the Ashtekar variables, with the densitized triads $E_i^a \equiv \sqrt{e} e_i^a$, curvature tensor $F_{ab}^i \equiv \partial_{[a} A_{b]}^i + \epsilon_{kl}^i A_l^k A_b^k$, and the Yang-Mills connection $A_a^i \equiv \Gamma_a^i + \gamma K_a^i$, the constraints of the BDT in the Yang-Mills phase space

read

$$\mathcal{G}_i = D_a E_i^a \approx 0, \quad (2.9)$$

$$\mathcal{V}_a = \frac{1}{\gamma} F_{ab}^i E_i^b + p_\phi \partial_a \phi \approx 0, \quad (2.10)$$

$$\begin{aligned} \mathcal{H} = & \frac{\phi}{2} \left[F_{ab}^j - \left(\gamma^2 + \frac{1}{\phi^2} \right) \epsilon_{jmn} \tilde{K}_a^m \tilde{K}_b^n \right] \frac{\epsilon_{jkl} E_k^a E_l^b}{\sqrt{q}} \\ & + \frac{1}{3+2w} \left[\frac{(\tilde{K}_a^i E_i^a)^2}{\phi \sqrt{q}} + 2 \frac{\tilde{K}_a^i E_i^a}{\sqrt{q}} p_\phi + \frac{p_\phi^2 \phi}{\sqrt{q}} \right] \\ & + \frac{w}{2\phi} \sqrt{q} (D_a \phi) D^a \phi + \sqrt{q} D_a D^a \phi \approx 0, \end{aligned} \quad (2.11)$$

which are often referred to as the Gauss, diffeomorphism and scalar constraints, respectively. In the above expressions, γ is the Barbero-Immirzi parameter and $\tilde{K}_a^i = e_i^b \tilde{K}_{ab}$ with

$$\tilde{K}^{ab} = \phi K^{ab} + \frac{q^{ab}}{2N} (\dot{\phi} - N^c \partial_c \phi). \quad (2.12)$$

In Eqs. (2.9)-(2.11), the symbol “ ≈ 0 ” indicates that the constraints hold only on the shell (hypersurface). Thus, the total Hamiltonian of BDT can be expressed as

$$C_{\text{total}} = \int d^3x (N^a \mathcal{V}_a + N \mathcal{H} + \mathcal{G}_i N^i). \quad (2.13)$$

III. SYMMETRY REDUCTION OF CLASSICAL BDT FOR BIANCHI I SPACETIMES

The four-dimensional Bianchi I spacetimes described by the metric

$$\begin{aligned} ds^2 = & -N^2 dt^2 + q_{ab} dx^a dx^b \\ = & -N^2 dt^2 + \sum_{I=1}^3 a_I^2 (dx_I)^2, \end{aligned} \quad (3.1)$$

have a topology of $\Sigma \times \mathbb{R}$, where N and a_I are functions of t only, $x^\mu \equiv (t, x^a)$ and $x^a \equiv (x, y, z)$. Thus, the intrinsic metric $q_{ab} = \text{diag}(a_1^2, a_2^2, a_3^2)$ defined on the spatial manifold Σ is homogeneous with three-dimensional symmetry group that is simply transitive. The symmetry of the spatial hypersurface is determined by the Killing vectors. Essentially, the Killing vector fields give the direction along which the metric does not change under the Lie dragging [43].

A. Classical Hamiltonian

Considering a fiducial cell with lengths L_1 , L_2 and L_3 along the three spatial directions [32],

$$ds_o^2 \equiv {}^o q_{ab} dx^a dx^b = dx_1^2 + dx_2^2 + dx_3^2, \quad (3.2)$$

its triads and cotriads, denoted, respectively, by \hat{e}_i^a and \hat{e}_a^i , satisfy the relations $\hat{e}_i^a \hat{e}_b^i = \delta_b^a$ and $\hat{e}_i^a \hat{e}_a^j = \delta_i^j$. Without loss of the generality, one often sets $L_1 = L_2 = L_3 \equiv l_0$, which will be adopted in this paper. The geometry of the Bianchi I spacetimes is one of the simplest types of Bianchi Class A models [63], such that it admits the Universe to have different scale factors in each principal direction, but with zero spatial curvature.

The introduction of fiducial triads trivializes the gauge freedom corresponding to the Gauss and the spatial diffeomorphisms constraints and they commute with the Killing vector fields denoted by $\hat{\xi}_i^a$, satisfying the relations $[\hat{e}_i, \hat{\xi}_j]^a = 0$. The underlying structure of the spatial hypersurface is dictated by the commutator relations, given by $[\hat{e}_i, \hat{e}_j]^a = C_{ij}^k \hat{e}_k^a$. The values of the structure constants C_{ij}^k completely define all the symmetry of the spatial sector. The Bianchi I model considered in this work is specified by $C_{jk}^i = 0$. To be specific, the Bianchi I hypersurface Σ is flat. Also, the homogeneity implies the contribution to the Hamiltonian from the spatial derivative is identically zero. The diagonal Bianchi I Universe in terms of the Ashtekar variables and densitized triads are parametrized by

$$A_a^i = \tilde{c}_i V_o^{-1/3} \hat{e}_i^a, \quad E_j^b = p_j V_o^{-2/3} \sqrt{q} \hat{e}_j^b, \quad (3.3)$$

which satisfy the canonical relations

$$\{A_a^i(x), E_j^b(y)\} = \gamma \delta_j^i \delta_a^b \delta(x-y), \quad (3.4)$$

where there is no summation over indexes i or j , and the volume of the fiducial cell V_o is given by $V_o = l_0^3$. Since Bianchi I spacetimes are homogeneous but anisotropic, \tilde{c}_i and p_j depend only on time. Also, since there is no spatial curvature, we have $\Gamma_a^i = 0$. As a result, the only constraint that survives after the adoption of the fiducial triad is the Hamiltonian constraint, which is given by

$$\begin{aligned} \mathcal{H} &= \frac{\phi}{2} \left[F_{ab}^j - \left(\gamma^2 + \frac{1}{\phi^2} \right) \epsilon_{jmn} \tilde{K}_a^m \tilde{K}_b^n \right] \frac{\epsilon_{jkl} E_k^a E_l^b}{\sqrt{q}} \\ &+ \frac{1}{3+2\omega} \left[\frac{(\tilde{K}_a^i E_i^a)^2}{\phi \sqrt{q}} + 2 \frac{(\tilde{K}_a^i E_i^a) p_\phi}{\sqrt{q}} + \frac{p_\phi^2}{\sqrt{q}} \right] \\ &+ \frac{\omega}{2\phi} \sqrt{q} (D_a \phi) D^a \phi + \sqrt{q} D_a D^a \phi. \end{aligned} \quad (3.5)$$

Since the Bianchi I spacetimes are spatially flat, $\Gamma_a^k = 0$, as pointed out, we find that

$$F_{ab}^j = \gamma^2 \epsilon_{kl}^j \tilde{K}_a^k \tilde{K}_b^l. \quad (3.6)$$

We also notice that for the parametrization (3.3), we have

$$\epsilon_{jkl} \epsilon_{jmn} E_k^a E_l^b \tilde{K}_a^m \tilde{K}_b^n = 2 E_m^a E_n^b \tilde{K}_{[a}^m \tilde{K}_{b]}^n, \quad (3.7)$$

$$\begin{aligned} E_m^a E_n^b \tilde{K}_{[a}^m \tilde{K}_{b]}^n &= \frac{\dot{q}}{\gamma^2 l_0^6} (\tilde{c}_1 \tilde{c}_2 p_1 p_2 + \tilde{c}_2 p_2 \tilde{c}_3 p_3 \\ &+ \tilde{c}_1 p_1 \tilde{c}_3 p_3), \end{aligned} \quad (3.8)$$

$$\tilde{K}_a^i E_i^a = \frac{\sqrt{q}}{\gamma l_0^3} (\tilde{c}_1 p_1 + \tilde{c}_2 p_2 + \tilde{c}_3 p_3), \quad (3.9)$$

where $[a, b] \equiv (ab - ba)/2$ denotes the antisymmetrization. In the limiting case of $\omega \rightarrow \infty$ and ϕ being a constant, the scalar constraint of the BDT gets reduced to the scalar constraint of Einstein's GR in the vacuum.

Now, combining all the terms and using that $\sqrt{q} = \sqrt{\dot{q}} \sqrt{p_1 p_2 p_3} / l_0^3$, we finally obtain

$$\begin{aligned} \mathcal{H} &= -\frac{\sqrt{q}}{l_0^3} \frac{1}{\sqrt{p_1 p_2 p_3}} \frac{1}{\gamma^2 \phi} \left[\tilde{c}_1 \tilde{c}_2 p_1 p_2 + \tilde{c}_2 p_2 \tilde{c}_3 p_3 + \tilde{c}_1 p_1 \tilde{c}_3 p_3 \right. \\ &\left. - \frac{1}{\beta} (\tilde{c}_1 p_1 + \tilde{c}_2 p_2 + \tilde{c}_3 p_3 + \gamma \pi_\phi \phi)^2 \right], \end{aligned} \quad (3.10)$$

where, in the move to homogeneous variables, we have redefined the conjugate momentum corresponding to the scalar field as $p_\phi \equiv \pi_\phi \sqrt{q} / l_0^3$ and $\beta = 3+2\omega$. The smeared Hamiltonian is obtained by integrating the symmetry reduced Hamiltonian, Eq. (3.10), over the fiducial volume V_0 , leading to

$$\begin{aligned} C_{\mathcal{H}} &= \int d^3x N \mathcal{H} \\ &= -\frac{N}{\sqrt{p_1 p_2 p_3}} \frac{1}{\gamma^2 \phi} \left[\tilde{c}_1 \tilde{c}_2 p_1 p_2 + \tilde{c}_2 p_2 \tilde{c}_3 p_3 + \tilde{c}_1 p_1 \tilde{c}_3 p_3 \right. \\ &\left. - \frac{1}{\beta} (\tilde{c}_1 p_1 + \tilde{c}_2 p_2 + \tilde{c}_3 p_3 + \gamma \pi_\phi \phi)^2 \right], \end{aligned} \quad (3.11)$$

where we have used $\int d^3x \sqrt{q} = l_0^3$.

B. Classical dynamics

The symplectic structure of the complete phase space in terms of the new variables reads

$$\{\tilde{c}_I, p_J\} = \gamma \delta_{IJ}, \quad (3.12)$$

$$\{\phi, \pi_\phi\} = 1. \quad (3.13)$$

The dynamics of a system is given by the Poisson equation, $\dot{\mathcal{O}} = \{\mathcal{O}, C_H\}$ for the phase space function \mathcal{O} . Then, the equations of motion for c_I and its conjugate variables p_I are

$$\dot{\tilde{c}}_I' = \gamma \delta_{IJ} \frac{\delta C_{\mathcal{H}}}{\delta p_J}, \quad (3.14)$$

$$p_I' = -\gamma \delta_{IJ} \frac{\delta C_{\mathcal{H}}}{\delta \tilde{c}_J}, \quad (3.15)$$

whereas the equations of motion for ϕ and its conjugate variable π_ϕ are

$$\dot{\phi}' = \frac{\delta C_{\mathcal{H}}}{\delta \pi_\phi}, \quad (3.16)$$

$$\pi_\phi' = -\frac{\delta C_{\mathcal{H}}}{\delta \phi}, \quad (3.17)$$

where a dot denotes the derivative with respect to cosmic time t and a prime denotes derivative with respect to τ defined as

$$d\tau \equiv N dt = \sqrt{p_1 p_2 p_3} dt. \quad (3.18)$$

In this work, we choose $N = \sqrt{p_1 p_2 p_3}$.

Using the Hamiltonian constraint, Eq. (3.11), we can now derive the equations of motion. In particular, from Eq. (3.14), we obtain the following equation of motion for the c_I variables,

$$\begin{aligned} \tilde{c}'_I &= -\frac{\tilde{c}_I}{\gamma\phi} \left[\tilde{c}_J p_J + \tilde{c}_K p_K \right. \\ &\quad \left. - \frac{2}{\beta} (\tilde{c}_I p_I + \tilde{c}_J p_J + \tilde{c}_K p_K + \gamma\pi_\phi\phi) \right], \end{aligned} \quad (3.19)$$

where $J, K \neq I$.

Similarly, from Eq. (3.15), we obtain the equation of motion for the conjugate variables p_I ,

$$\begin{aligned} p'_I &= \frac{p_I}{\gamma\phi} \left[\tilde{c}_J p_J + \tilde{c}_K p_K \right. \\ &\quad \left. - \frac{2}{\beta} (\tilde{c}_I p_I + \tilde{c}_J p_J + \tilde{c}_K p_K + \gamma\pi_\phi\phi) \right]. \end{aligned} \quad (3.20)$$

Finally, from Eqs. (3.16) and (3.17), respectively, the equations of motion for the BD scalar field ϕ and its conjugate momentum π_ϕ are given by

$$\phi' = \frac{2}{\beta\gamma} (\tilde{c}_1 p_1 + \tilde{c}_2 p_2 + \tilde{c}_3 p_3 + \gamma\pi_\phi\phi), \quad (3.21)$$

$$\begin{aligned} \pi'_\phi &= -\frac{1}{\gamma^2\phi^2} \left\{ (\tilde{c}_1 p_1 \tilde{c}_2 p_2 + \tilde{c}_2 p_2 \tilde{c}_3 p_3 + \tilde{c}_1 p_1 \tilde{c}_3 p_3) \right. \\ &\quad \left. - \frac{1}{\beta} [(\tilde{c}_1 p_1 + \tilde{c}_2 p_2 + \tilde{c}_3 p_3)^2 - (\phi\gamma\pi_\phi)^2] \right\}. \end{aligned} \quad (3.22)$$

The set of Eqs. (3.19)-(3.22) completely specifies the classical dynamics of the Bianchi-I spacetimes for BDT. Note that even at the level of equations of motion, it is straightforward to see that in the limit $\omega \rightarrow \infty$ and constant ϕ , the equations of motion for the Einstein-Hilbert action are recovered [43].

IV. LOOP QUANTUM EFFECTIVE DYNAMICS OF BIANCHI I SPACETIMES IN BDT

The loop effective quantum dynamics for homogeneous and isotropic Universe in LQC [64] have been studied extensively, and now it is well established [12] that the effective dynamics incorporate the leading-order quantum geometric effects of the full theory very well even in the deep Planck regime [65]. This is especially true for the states that are sharply peaked on a classical trajectory at late times [66].

In the homogeneous and isotropic FLRW Universe, it is obtained by the replacement

$$c \rightarrow \frac{\sin(\mu c)}{\mu},$$

where c denotes the conjugate momentum of the area operator p ($\propto a^2$, where a is the expansion factor of the Universe), and the lattice spacing, μ , is called the polymerization parameter. Different choices of the parameter

μ give rise to different schemes of quantization with distinct effective dynamics. The expectation is that this would act as an ultraviolet regulator and mitigate the initial singularity [67, 68].

In the literature, various choices of μ have been considered [12, 69]¹. In particular, in the original scheme—the μ_o scheme [71], the area gap was implemented as a kinematic feature on the comoving frame, which is equivalent to introducing a fixed lattice of constant spacing, so that the area \square_{ij} in the (i, j) plane is measured by the fiducial metric ${}^oq_{ab}$ defined by Eq. (3.2). However, it was found that this leads to inconsistencies [72]. After extensive investigations in the past two decades or so (see, for example, Ref. [69] and references therein), it was found that the $\bar{\mu}$ scheme [73], which is sometimes also referred to as improved dynamics, is the unique one that leads to consistent physics not only for the homogeneous and isotropic quantum background, but also for its linear perturbations [12, 13, 15, 16]. The distinguishable feature of the $\bar{\mu}$ scheme comes from the observation that the quantization of area should refer to physical geometries instead of the fiducial metric. In particular, the area \square_{ij} in the (i, j) plane should be measured by the physical metric q_{ab} defined in Eq. (3.1), instead of the fiducial metric ${}^oq_{ab}$ defined by Eq. (3.2). Since the physical area of the faces of an elementary cell is p , and each side of \square_{ij} is $\sqrt{\Delta}$ times the edge of the elementary cell, we are led to [73]

$$\bar{\mu}^2 p = \Delta \quad \Rightarrow \quad \bar{\mu} = \sqrt{\frac{\Delta}{p}}, \quad (4.1)$$

where $\Delta \equiv 4\pi\sqrt{3}\gamma l_{Pl}^2$ is the area gap in the full theory of LQG [7].

When generalizing the above $\bar{\mu}$ scheme to the homogeneous but anisotropic cases, including the Bianchi I models, in the literature there exist two different schemes [28–30, 32], which we shall introduce below and refer them to as the $\bar{\mu}_A$ and $\bar{\mu}_B$ schemes, respectively. Both schemes have been studied in great details [33–47], and showed that, among other interesting features, the singularities are resolved and replaced by quantum bounces. More recently [47], it was found that the $\bar{\mu}_A$ quantization suffers from a problem in which one of the triad components and associated polymerized term retains Planckian character even at large volumes. As a result, not only is the anisotropic shear not preserved across the bounce, but also the Universe can exhibit an unexpected cyclic evolution.

¹ It should be noted that the choices of μ are purely geometric and are independent of the underlying theory. As a result, they are applicable to the Brans-Dicke theory considered in this paper. For more details, see Ref. [70] and references therein.

A. The $\bar{\mu}_A$ quantization scheme

The $\bar{\mu}_A$ scheme, proposed in Ref. [28], for the homogeneous and anisotropic Bianchi I model is specified by

$$\bar{\mu}_I = \sqrt{\frac{\Delta}{p_I}}. \quad (4.2)$$

Clearly, when $p_I \gg \Delta$, we have $\bar{\mu}_I \rightarrow 0$, and expect that the quantum effects are very small and the classical

limit is obtained. However, near the singular point, $p_I \simeq 0$, we have $\bar{\mu}_I \gg 1$, such that the quantum effects are expected to be very large. In the following, we shall consider whether such effects are larger enough so that the spacetime singularity that used to appear classically at $p_I = 0$ will now be regulated in the current setup.

Returning to our model under investigation, from Eq. (3.11), the quantum deformed Hamiltonian constraint becomes

$$C_{\text{eff}} = -\frac{1}{\gamma^2\phi} \left[\frac{\sin(\bar{\mu}_1\tilde{c}_1)}{\bar{\mu}_1} p_1 \frac{\sin(\bar{\mu}_2\tilde{c}_2)}{\bar{\mu}_2} p_2 + \frac{\sin(\bar{\mu}_2\tilde{c}_2)}{\bar{\mu}_2} p_2 \frac{\sin(\bar{\mu}_3\tilde{c}_3)}{\bar{\mu}_3} p_3 + \frac{\sin(\bar{\mu}_3\tilde{c}_3)}{\bar{\mu}_3} p_3 \frac{\sin(\bar{\mu}_1\tilde{c}_1)}{\bar{\mu}_1} p_1 \right] \\ + \frac{1}{\beta\gamma^2\phi} \left[\frac{\sin(\bar{\mu}_1\tilde{c}_1)}{\bar{\mu}_1} p_1 + \frac{\sin(\bar{\mu}_2\tilde{c}_2)}{\bar{\mu}_2} p_2 + \frac{\sin(\bar{\mu}_3\tilde{c}_3)}{\bar{\mu}_3} p_3 + \gamma\pi_\phi\phi \right]^2 + \frac{P_\Phi^2}{2}. \quad (4.3)$$

Note that, in order to study the effective theory of loop quantum Brans-Dicke cosmology, we also want to know the effect of matter fields on the dynamical evolution. Hence, we have included in Eq. (4.3) an extra massless scalar matter field Φ , with momentum conjugate P_Φ , and the corresponding energy density is given by

$$\rho = \frac{P_\Phi^2}{2p_1p_2p_3}. \quad (4.4)$$

Since C_{eff} does not depend explicitly on the scalar field

Φ , we have

$$P'_\Phi = -\frac{\partial C_{\text{eff}}}{\partial \Phi} = 0, \quad (4.5)$$

that is, P_Φ is a constant of motion. On the other hand, the other quantum corrected Hamilton's equations for the symmetry reduced connection parametrized by \tilde{c} with the $\bar{\mu}_A$ scheme given by Eq. (4.2) are given by

$$\tilde{c}'_I = -\frac{1}{\gamma\phi} \left[\frac{3\sin(\bar{\mu}_I\tilde{c}_I)}{2\bar{\mu}_I} - \frac{c_I \cos(\bar{\mu}_I\tilde{c}_I)}{2} \right] \left\{ \frac{\sin(\bar{\mu}_J\tilde{c}_J)}{\bar{\mu}_J} p_J + \frac{\sin(\bar{\mu}_K\tilde{c}_K)}{\bar{\mu}_K} p_K \right. \\ \left. - \frac{2}{\beta} \left[\frac{\sin(\bar{\mu}_I\tilde{c}_I)}{\bar{\mu}_I} p_I + \frac{\sin(\bar{\mu}_J\tilde{c}_J)}{\bar{\mu}_J} p_J + \frac{\sin(\bar{\mu}_K\tilde{c}_K)}{\bar{\mu}_K} p_K + \gamma\pi_\phi\phi \right] \right\} \\ + \gamma p_J p_K \left(\rho + p_I \frac{\partial \rho}{\partial p_I} \right). \quad (4.6)$$

For other choices of schemes for $\bar{\mu}_I$, the change will be in the terms inside the first square brackets. Similarly, quantum corrected equations of motion for the symmetry reduced densitized triads parametrized by p_I are given by

$$p'_I = \frac{p_I}{\phi\gamma} \cos(\bar{\mu}_I\tilde{c}_I) \left\{ \frac{\sin(\bar{\mu}_J\tilde{c}_J)}{\bar{\mu}_J} p_J + \frac{\sin(\bar{\mu}_K\tilde{c}_K)}{\bar{\mu}_K} p_K \right. \\ \left. - \frac{2}{\beta} \left[\frac{\sin(\bar{\mu}_I\tilde{c}_I)}{\bar{\mu}_I} p_I + \frac{\sin(\bar{\mu}_J\tilde{c}_J)}{\bar{\mu}_J} p_J \right. \right. \\ \left. \left. + \frac{\sin(\bar{\mu}_K\tilde{c}_K)}{\bar{\mu}_K} p_K + \gamma\pi_\phi\phi \right] \right\}. \quad (4.7)$$

Finally, the equations of motion for ϕ and its conjugate

momentum π_ϕ read

$$\phi' = \frac{2}{\gamma\beta} \left[\frac{\sin(\tilde{c}_1\bar{\mu}_1)}{\bar{\mu}_1} p_1 + \frac{\sin(\tilde{c}_2\bar{\mu}_2)}{\bar{\mu}_2} p_2 + \frac{\sin(\tilde{c}_3\bar{\mu}_3)}{\bar{\mu}_3} p_3 \right. \\ \left. + \gamma\pi_\phi\phi \right], \quad (4.8) \\ \pi'_\phi = -\frac{1}{\gamma^2\phi^2} \left\{ \frac{\sin(\bar{\mu}_1\tilde{c}_1)}{\bar{\mu}_1} p_1 \frac{\sin(\bar{\mu}_2\tilde{c}_2)}{\bar{\mu}_2} p_2 \right. \\ \left. + \frac{\sin(\bar{\mu}_2\tilde{c}_2)}{\bar{\mu}_2} p_2 \frac{\sin(\bar{\mu}_3\tilde{c}_3)}{\bar{\mu}_3} p_3 + \frac{\sin(\bar{\mu}_1\tilde{c}_1)}{\bar{\mu}_1} p_1 \frac{\sin(\bar{\mu}_3\tilde{c}_3)}{\bar{\mu}_3} p_3 \right. \\ \left. + \frac{(\gamma\pi_\phi\phi)^2}{\beta} \right. \\ \left. - \frac{1}{\beta} \left(\frac{\sin(\tilde{c}_1\bar{\mu}_1)}{\bar{\mu}_1} p_1 + \frac{\sin(\tilde{c}_2\bar{\mu}_2)}{\bar{\mu}_2} p_2 + \frac{\sin(\tilde{c}_3\bar{\mu}_3)}{\bar{\mu}_3} p_3 \right)^2 \right\}. \quad (4.9)$$

The set of Eqs. (4.6)-(4.9) completely define the quantum corrected dynamics of the Bianchi-I spacetime in $\bar{\mu}_A$ scheme for BDT in the Jordan's frame.

Once the above equations are solved, we can compute the average Hubble parameter H and the expansion factor a for the effective quantum Bianchi-I spacetime

$$H \equiv \frac{H_1 + H_2 + H_3}{3}, \quad a \equiv \sqrt{a_1 a_2 a_3}, \quad (4.10)$$

where $H_I = \dot{a}_I/a_I$ and $p_I = a_J a_K l_0^2$ for nonrepeated indexes I, J, K . In particular, the average Hubble parameter reads

$$\begin{aligned} H = & \frac{1}{6\gamma\phi\sqrt{p_1 p_2 p_3}} \left\{ \left[\frac{\sin(\bar{\mu}_2 \tilde{c}_2)}{\bar{\mu}_2} p_2 + \frac{\sin(\bar{\mu}_3 \tilde{c}_3)}{\bar{\mu}_3} p_3 \right] \right. \\ & \times \cos(\bar{\mu}_1 \tilde{c}_1) \\ & + \left[\frac{\sin(\bar{\mu}_1 \tilde{c}_1)}{\bar{\mu}_1} p_1 + \frac{\sin(\bar{\mu}_3 \tilde{c}_3)}{\bar{\mu}_3} p_3 \right] \cos(\bar{\mu}_2 \tilde{c}_2) \\ & \left. + \left[\frac{\sin(\bar{\mu}_2 \tilde{c}_2)}{\bar{\mu}_2} p_2 + \frac{\sin(\bar{\mu}_1 \tilde{c}_1)}{\bar{\mu}_1} p_1 \right] \cos(\bar{\mu}_3 \tilde{c}_3) \right\} \\ & - \frac{\dot{\phi}}{6\phi\sqrt{p_1 p_2 p_3}} [\cos(\bar{\mu}_1 \tilde{c}_1) + \cos(\bar{\mu}_2 \tilde{c}_2) + \cos(\bar{\mu}_3 \tilde{c}_3)], \end{aligned} \quad (4.11)$$

where the factor $\sqrt{p_1 p_2 p_3}$ comes from Eq. (3.18). To see how classical singularities can be avoided in the framework of LQG, let us provide some heuristic arguments, by following the analysis provided in [29]. For more details, see our numerical analyses to be presented in the next section.

Defining

$$\mathcal{G}_I(t') = p_I \frac{\sin(\bar{\mu}_I \tilde{c}_I)}{\bar{\mu}_I}, \quad (4.12)$$

and using Eqs. (4.6)-(4.7), one can show that

$$\mathcal{G}'_I(t') = \gamma \cos(\bar{\mu}_I \tilde{c}_I) p_1 p_2 p_3 \left(\rho + p_I \frac{\partial \rho}{\partial p_I} \right). \quad (4.13)$$

Now setting the quantum effective constraint, Eq. (4.3), to zero, one obtains

$$\gamma^2 p_1 p_2 p_3 \rho_{\text{eff}} = \mathcal{G}_1 \mathcal{G}_2 + \mathcal{G}_2 \mathcal{G}_3 + \mathcal{G}_1 \mathcal{G}_3, \quad (4.14)$$

$$\begin{aligned} & - \frac{1}{\gamma^2 \phi} \left[\frac{\sin(\bar{\mu}_1 \tilde{c}_1)}{\bar{\mu}_1} p_1 \frac{\sin(\bar{\mu}_2 \tilde{c}_2)}{\bar{\mu}_2} p_2 + \frac{\sin(\bar{\mu}_2 \tilde{c}_2)}{\bar{\mu}_2} p_2 \frac{\sin(\bar{\mu}_3 \tilde{c}_3)}{\bar{\mu}_3} p_3 + \frac{\sin(\bar{\mu}_3 \tilde{c}_3)}{\bar{\mu}_3} p_3 \frac{\sin(\bar{\mu}_1 \tilde{c}_1)}{\bar{\mu}_1} p_1 \right] \\ & + \frac{1}{\beta \gamma^2 \phi} \left[\frac{\sin(\bar{\mu}_1 \tilde{c}_1)}{\bar{\mu}_1} p_1 + \frac{\sin(\bar{\mu}_2 \tilde{c}_2)}{\bar{\mu}_2} p_2 + \frac{\sin(\bar{\mu}_3 \tilde{c}_3)}{\bar{\mu}_3} p_3 + \gamma \pi_\phi \phi \right]^2 + p_1 p_2 p_3 \rho = 0. \end{aligned} \quad (4.20)$$

Note that in the second line of the above equation the term in the square brackets can be written in terms of

where we have used Eq. (4.8) and defined the effective energy density as

$$\rho_{\text{eff}} = \frac{\beta \dot{\phi}^2}{4} + \rho \phi. \quad (4.15)$$

Since ρ is given by Eq. (4.4), we find the identity

$$\rho + p_I \frac{\partial \rho}{\partial p_I} = 0, \quad (4.16)$$

which means that \mathcal{G}_I are constants. For constant \mathcal{G}_I , from Eq. (4.12), given that the sines have a maximum value of unit, it sets a lower bound on p_I ,

$$p_I \geq (|\mathcal{G}_I| \sqrt{\Delta})^{2/3}. \quad (4.17)$$

This is to say that the results of Ref. [29] also hold in the present case of BDT, provided that $\rho \rightarrow \rho_{\text{eff}}$. Then Eq. (4.17) shows that all scale factors are bounded from below, which proves that a nonsingular behavior is present.

B. The $\bar{\mu}_B$ quantization scheme

In the $\bar{\mu}_B$ scheme, we have [40]

$$\bar{\mu}_I = \sqrt{\frac{\Delta p_I}{p_J p_K}}, \quad (4.18)$$

where I, J , and K are nonrepeated indexes. The corresponding effective Hamiltonian takes the same form as that given by Eq. (4.3). Following the same steps provided in the last subsection, we can obtain the corresponding Hamiltonian equations. In particular, it can be shown that

$$\begin{aligned} \dot{\phi}^2 = & \frac{4}{\gamma^2 \beta^2 (p_1 p_2 p_3)} \left[\frac{p_1 \sin(\tilde{c}_1 \bar{\mu}_1)}{\bar{\mu}_1} + \frac{p_2 \sin(\tilde{c}_2 \bar{\mu}_2)}{\bar{\mu}_2} \right. \\ & \left. + \frac{p_3 \sin(\tilde{c}_3 \bar{\mu}_3)}{\bar{\mu}_3} + \gamma \pi_\phi \phi \right]^2, \end{aligned} \quad (4.19)$$

which is now written with respect to the cosmic time t . Now setting once again the quantum effective Hamiltonian constraint, Eq. (4.3), to zero, one obtains

Eq. (4.19), then one obtains

$$\begin{aligned} \frac{\beta \dot{\phi}^2}{4\phi} + \rho = & \frac{1}{\gamma^2 \phi} \left[\frac{\sin(\bar{\mu}_1 \tilde{c}_1) \sin(\bar{\mu}_2 \tilde{c}_2)}{\bar{\mu}_1 \bar{\mu}_2 p_3} \right. \\ & \left. + \frac{\sin(\bar{\mu}_2 \tilde{c}_2) \sin(\bar{\mu}_3 \tilde{c}_3)}{\bar{\mu}_2 \bar{\mu}_3 p_1} + \frac{\sin(\bar{\mu}_3 \tilde{c}_3) \sin(\bar{\mu}_1 \tilde{c}_1)}{\bar{\mu}_1 \bar{\mu}_3 p_2} \right]. \end{aligned} \quad (4.21)$$

At this point, we apply the aforementioned alternative scheme, given by Eq. (4.18), in Eq. (4.21), and define an effective energy density ρ_{eff} as

$$\begin{aligned} \frac{\rho_{\text{eff}}}{\rho_c} &\equiv \frac{\gamma^2 \Delta}{3} \left(\frac{\beta \dot{\phi}^2}{4} + \rho \phi \right) \\ &= \frac{1}{3} \left[\sin(\bar{\mu}_1 \tilde{c}_1) \sin(\bar{\mu}_2 \tilde{c}_2) + \sin(\bar{\mu}_2 \tilde{c}_2) \sin(\bar{\mu}_3 \tilde{c}_3) \right. \\ &\quad \left. + \sin(\bar{\mu}_1 \tilde{c}_1) \sin(\bar{\mu}_3 \tilde{c}_3) \right]. \end{aligned} \quad (4.22)$$

Clearly, such defined effective energy density is bounded from above by its maximal value ρ_c , given by $\rho_c = 3/(\gamma^2 \Delta)$. These results are in agreement with Ref. [74] in the isotropic limit.

Now, a maximal value of energy density implies a minimum value of spatial volume. Therefore, initializing the Universe with a contracting phase, a quantum bounce is predicted in this scenario. This confirms the removal of an initial singularity in the framework of LQG owing to the fact that geometry is quantized and there exists a nonzero minimal area gap. Starting with an initially contracting phase, in a classical setup, the collapse will inevitably lead to a spacetime singularity. Thus, once again, through this analysis we conclude that quantum geometric effects at the Planck scale provide repulsive forces and replace classical spacetime singularities by nonsingular quantum bounces.

For completeness, let us now write a closed form of the modified Friedmann equation and that can be derived using the current scheme. From Eqs. (4.11) and (4.19), we obtain that

$$\begin{aligned} \left(H + \frac{\dot{\phi}}{2\phi} \right)^2 &= \left\{ \frac{1}{6\gamma\sqrt{\Delta}\phi} \left[\sin(\tilde{c}_1 \bar{\mu}_1) \cos(\tilde{c}_2 \bar{\mu}_2) + \sin(\tilde{c}_2 \bar{\mu}_2) \cos(\tilde{c}_1 \bar{\mu}_1) + \sin(\tilde{c}_1 \bar{\mu}_1) \cos(\tilde{c}_3 \bar{\mu}_3) + \sin(\tilde{c}_3 \bar{\mu}_3) \cos(\tilde{c}_1 \bar{\mu}_1) \right. \right. \\ &\quad \left. \left. + \sin(\tilde{c}_2 \bar{\mu}_2) \cos(\tilde{c}_3 \bar{\mu}_3) + \sin(\tilde{c}_3 \bar{\mu}_3) \cos(\tilde{c}_2 \bar{\mu}_2) \right] + \frac{\dot{\phi}}{2\phi} \left[1 - \frac{\cos(\tilde{c}_1 \bar{\mu}_1) + \cos(\tilde{c}_2 \bar{\mu}_2) + \cos(\tilde{c}_3 \bar{\mu}_3)}{3} \right] \right\}^2. \end{aligned} \quad (4.23)$$

Inspired by Eq. (4.22), we define the directional effective energy density in the I direction as

$$\rho_{\text{eff}}^{(I)} = \frac{3 \sin^2(\tilde{c}_I \bar{\mu}_I)}{\gamma^2 \Delta}. \quad (4.24)$$

Using this definition, Eq. (4.23) can now be expressed as

$$\begin{aligned} \left(H + \frac{\dot{\phi}}{2\phi} \right)^2 &= \left\{ \frac{1}{6\phi} \left[\sqrt{\frac{1}{3} \rho_{\text{eff}}^{(1)} \left(1 - \frac{\rho_{\text{eff}}^{(2)}}{\rho_c} \right)} + \sqrt{\frac{1}{3} \rho_{\text{eff}}^{(2)} \left(1 - \frac{\rho_{\text{eff}}^{(1)}}{\rho_c} \right)} + \sqrt{\frac{1}{3} \rho_{\text{eff}}^{(1)} \left(1 - \frac{\rho_{\text{eff}}^{(3)}}{\rho_c} \right)} \right. \right. \\ &\quad \left. \left. + \sqrt{\frac{1}{3} \rho_{\text{eff}}^{(3)} \left(1 - \frac{\rho_{\text{eff}}^{(1)}}{\rho_c} \right)} + \sqrt{\frac{1}{3} \rho_{\text{eff}}^{(2)} \left(1 - \frac{\rho_{\text{eff}}^{(3)}}{\rho_c} \right)} + \sqrt{\frac{1}{3} \rho_{\text{eff}}^{(3)} \left(1 - \frac{\rho_{\text{eff}}^{(2)}}{\rho_c} \right)} \right] \right. \\ &\quad \left. + \frac{\dot{\phi}}{2\phi} \left[1 - \frac{1}{3} \left(\sqrt{1 - \frac{\rho_{\text{eff}}^{(1)}}{\rho_c}} + \sqrt{1 - \frac{\rho_{\text{eff}}^{(2)}}{\rho_c}} + \sqrt{1 - \frac{\rho_{\text{eff}}^{(3)}}{\rho_c}} \right) \right] \right\}^2. \end{aligned} \quad (4.25)$$

The above equation reduces to the isotropic BD theory [74] in the limit where the directional effective energy densities are equal. Also, the effective Friedmann equation of LQC is recovered for $\phi = 1$, when $\rho_{\text{eff}} \rightarrow \rho$.

V. DYNAMICS OF BIANCHI I UNIVERSE

In this section we present our numerical results for the effective dynamics of the models considered in the last section. We show the evolution of the scale factors and

Hubble parameters of the Bianchi I Universe for LQC and BDT in each of the quantization schemes. To be able to compare our results with the ones obtained in Ref. [47] in the framework of LQC, here we choose the same initial conditions as those used by the authors of that reference. On the other hand, in the framework of BDT, we choose the initial condition for the triad and the connection variables as close as possible to those in LQC. In particular, in all of our numerical results for LQC, we choose the initial conditions $c_1 = -0.13$, $c_2 = -0.12$, $p_1 = 10^3$, $p_2 = 2 \times 10^3$, $p_3 = 3 \times 10^3$, while c_3 is determined from the Hamiltonian constraint, Eq. (4.20),

with $(\phi, \dot{\phi}, \rho) = (1, 0, 0)$.

With the above in mind, in Figs. 1 and 2 we show our numerical results for the directional scale factors a_I ($I = 1, 2, 3$) of the Bianchi-I spacetimes, in both LQC and BDT, for the $\bar{\mu}_A$ and $\bar{\mu}_B$ schemes, given, respectively by Eqs. (4.2) and (4.18), with the parameters described in the figure captions. Each figure has four panels for

each scheme. Figures 1(a) and 2(a) shows the results for the LQC model, while Figs. 1(b)-1(d) and 2(b)-2(d) show the results for the BDT models. Notice that we use initial conditions for $\dot{\phi}$ instead of π_ϕ because it is more transparent when considering the limit $\text{BDT} \rightarrow \text{LQC}$, which happens for $(\phi, \dot{\phi}) \rightarrow (1, 0)$.

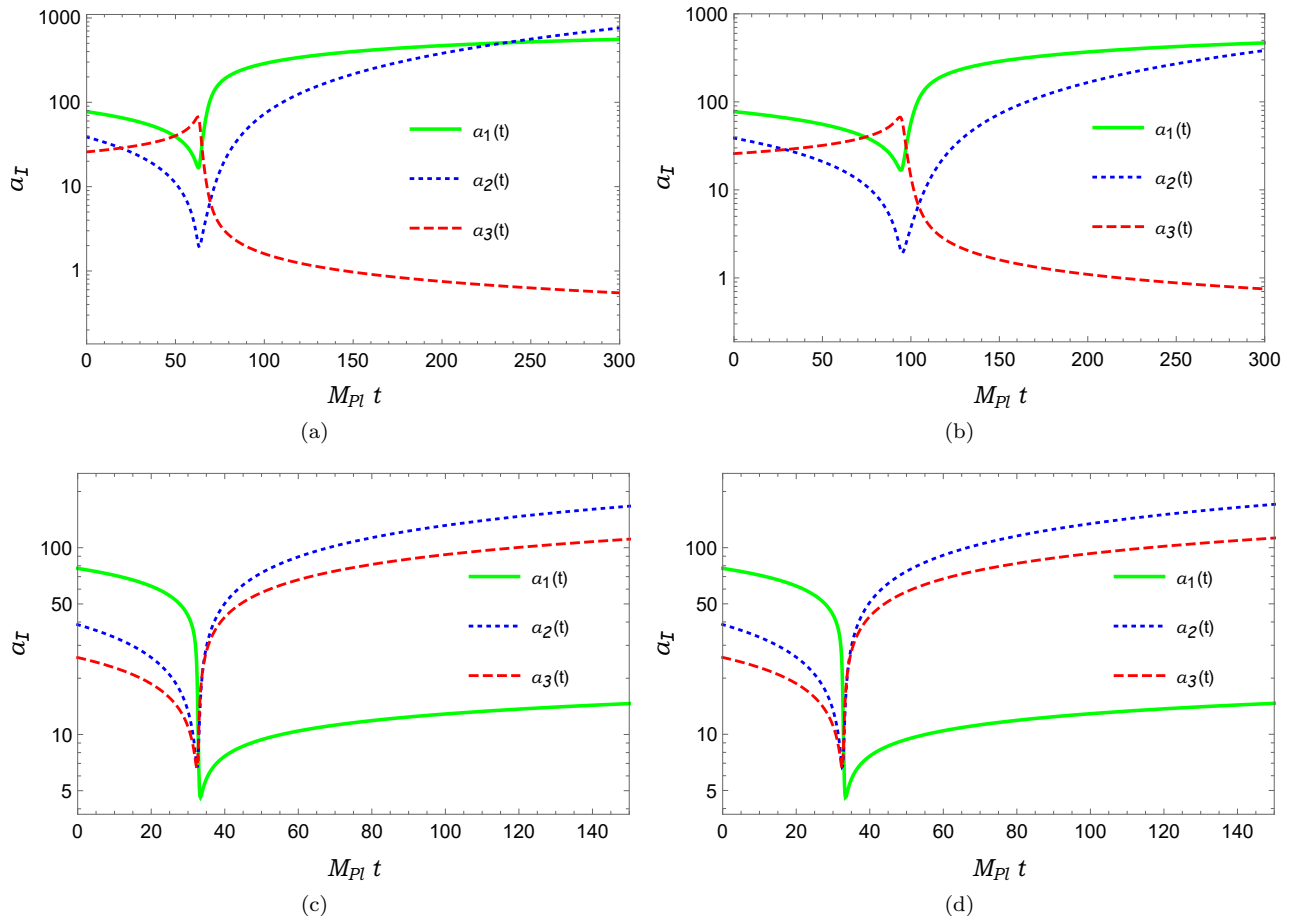


FIG. 1. The evolution of the directional scale factors a_I ($I = 1, 2, 3$) of the Bianchi-I spacetimes, where (a) is for LQC and (b) - (d) are for BDT. The initial conditions for LQC are $c_1 = -0.13$, $c_2 = -0.12$, $p_1 = 10^3$, $p_2 = 2 \times 10^3$, $p_3 = 3 \times 10^3$. For BDT, we adopt the same initial conditions as those of LQC with the addition of $(\phi, \dot{\phi}) = (1.5, 0)$ for (b), $(\phi, \dot{\phi}) = (1.0, 5.5 \times 10^{-5})$ for Panel (c), and $(\phi, \dot{\phi}) = (1.0, -5.5 \times 10^{-5})$ for (d), respectively, and set $\omega = 2 \times 10^5$ [58] for the BD parameter in all these three last. All plots correspond to the $\bar{\mu}_A$ scheme.

In Figs. 1(a) and 2(a) we show the results for the directional scale factors a_I ($I = 1, 2, 3$) of the Bianchi-I spacetime in the framework of LQC for the $\bar{\mu}_A$ and $\bar{\mu}_B$ schemes, respectively. Comparing them with the corresponding ones given in Ref. [47], one can see clearly the

consistency among these figures within the numerical errors. As a result, the numerical code used in the current paper and the one used in Ref. [47] are all reliable and give the same results.

Then, comparing Fig. 1(a) with Fig. 1(b), we can see

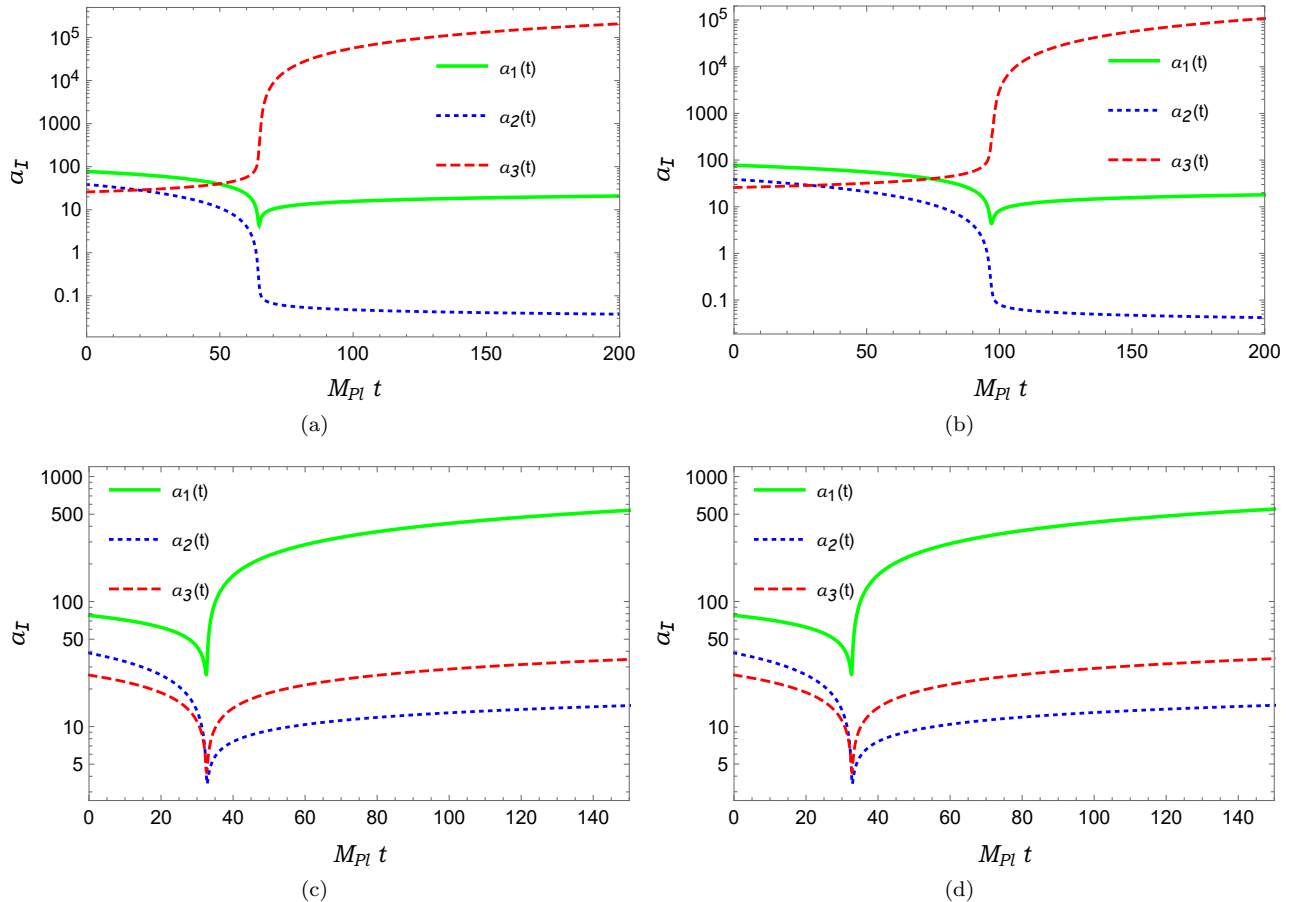


FIG. 2. The same as in Fig. 1, but for the $\bar{\mu}_B$ scheme.

that the deviations of BDT from that of LQC are simply the delay of the bounce in each direction, while the main qualitative behavior is preserved. This is because in the present case the initial condition of $\dot{\phi}$ is chosen to be zero, as that in LQC, so at the beginning the BDT effects are negligible. This type of dynamics is consistent with a Kasner-like phase, i.e., expansion followed by contraction in one direction and contraction followed by expansion in the others. It is important to note that even though there appears contraction in one of the three directions, we have checked explicitly that it never reaches zero (e.g., reaches a spacetime singularity) in that direction, but it always reaches asymptotically a nonzero value. Similar behavior has been also observed previously in LQC, see, for example, Refs. [29] [30] [47]. From the numerical studies that we have performed, we have also verified that the inclusion of a massless scalar field Φ does not change the results significantly, as long as $\dot{\phi}(t_i) = 0$, where t_i denotes the initial time.

However, from Fig. 1(c) we can see that once the initial condition of $\dot{\phi}$ is different from zero, the deviations become significant. In particular, all the three directional scale factors are increasing after the bounce (at $M_{Pl}t_B \simeq 33$) and soon after the bounce they become

comparable with their initial values. This is sharply in contrast to the LQC case (first seen in Ref. [47]), in which one of the three directional scale factors is always decreasing, and only two of them are increasing after the bounce. Here we see that this is also true for both μ_A and μ_B schemes when $\dot{\phi} = 0$, as one can see from Figs. 1(b) and 2(b). On the other hand, the difference between Figs. 1(c) and 1(d) is the choice of the sign of $\dot{\phi}$ at the initial moment. In fact, in Fig. 1(c) we chose $(\phi, \dot{\phi}) = (1.0, 5.5 \times 10^{-5})$, while in Fig. 1(d) we chose $(\phi, \dot{\phi}) = (1.0, -5.5 \times 10^{-5})$. The results for both cases show that the directional scale factors remain the same. This can be seen from Eq. (4.14), in which its right-hand side is a constant, while its left-hand side is independent of the signs of $\dot{\phi}$, as one can see from Eq. (4.15). Recall that $p_I \equiv l_0^2 a_J a_K$ for nonrepeated indexes I, J, K . Similar results as the ones for the μ_A scheme are also seen for the μ_B schemes. Comparing Fig. 2(a) with Fig. 2(b), we can see that the directional scale factors behave quite similar, modulated the simple delay of the bounce in each direction. In particular, only two of the three directional scale factors are increasing after the bounce, while the third one is always decreasing, which is again consistent as the results observed in Ref. [47]. Again, this is because

of the choice of the initial condition $\dot{\phi}(t_i) = 0$, which is initially identical to those in the LQC case. However, once $\dot{\phi}(t_i) \neq 0$, as shown explicitly in Figs. 2(c) and 2(d), the deviations become large. Remarkably, all the three directional scale factors are increasing right after the bounce and soon become comparable with their initial values. That is, if the evolution of the spacetime starts from a classical point, it will collapse to a minimal but nonzero volume, where the quantum bounce occurs and replaces the classical spacetime singularity by a finite quantum bounce. Afterwards, the spacetime starts to expand in each of the three directions, and soon approaches to a size that is comparable with the initial one. This is true not only in terms of volumes and areas but also in terms of the size in each of the three directions. This is dramatically different from that observed in LQC for the μ_A scheme [47].

To understand the properties of the models further, in Figs. 3 and 4, we show the numerical results for the average scale factor a and Hubble parameter H , defined by Eq. (4.10), for both of the μ_A and μ_B schemes. In each of these figures, the initial conditions are chosen the same as the corresponding ones given in Figs. 1 and 2, respectively, for the μ_A and μ_B schemes. In particular, Figs. 3 and 4 show similar behaviors for the LQC models as presented in Refs. [30, 47], while for the BDT models, the effects of the BD scalar $\dot{\phi}$ depend on the choice of the initial conditions. When $\dot{\phi}(t_i) = 0$, the effects with respect to LQC are simply to delay the bounce, and make the increase of the scale factor slower, while for the initial conditions with $\dot{\phi}(t_i) \neq 0$, the effects are opposite, that is, the bounce happens earlier, and the average scale factor increases faster after the bounce. Again, such behaviors do not depend on the signs of $\dot{\phi}(t_i)$ for the same reasons as explained above for the directional scale factors a_I 's. Hence, the results for the same absolute value of $\dot{\phi}(t_i)$ are overlapping.

Note that an overall behavior of the average Hubble parameter is also consistent with the results obtained earlier in Ref. [54], although the effects of the initial conditions on the shapes of a and H were not considered there.

In addition, in all the figures we have plotted the curves only up to $M_{Pl}t \lesssim 300$, but we have found that the asymptotical behavior of the curves remains the same. In fact, we have run our codes up to $M_{Pl}t \simeq 10^6$ and found no changes. So, their asymptotical behavior remains the same.

Analysis of these figures leads us to conclude that, for the representative parameters and initial conditions considered, all results consistently demonstrate that the classical singularity is replaced by a regular quantum bounce. In the absence of BD effects, this bounce occurs around $t = 65/M_{Pl}$. However, the BD effects can shift the bounce to earlier or later times depending on the initial conditions of the BD scalar $\phi(t_i)$ and its derivative $\dot{\phi}(t_i)$, where t_i denotes the initial time. Furthermore, the BD effects prevent the suppression of the directional scale factors after the bounce, a stark contrast to what

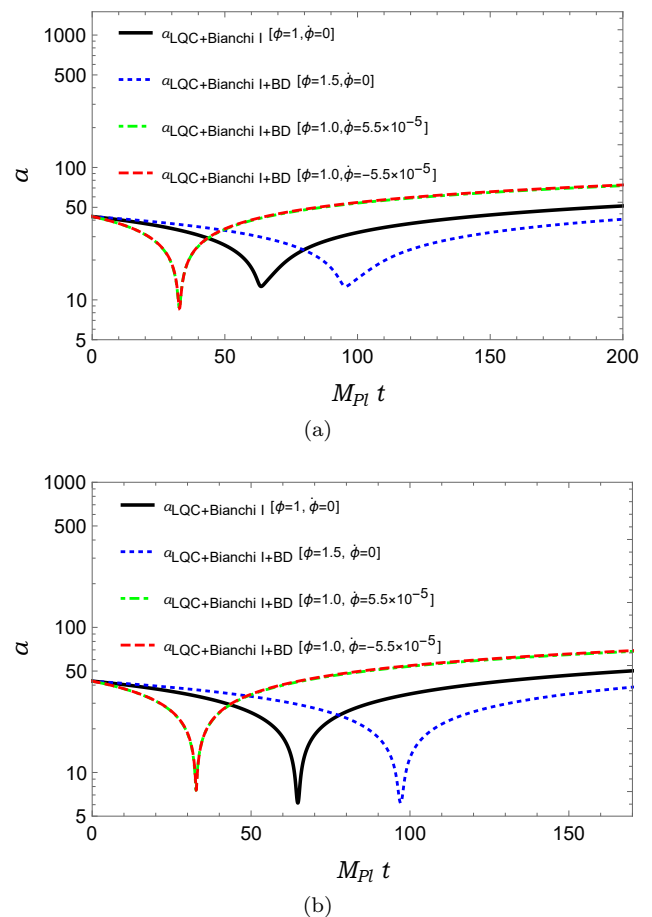


FIG. 3. The average scale factor a of the Bianchi I spacetime for the μ_A [(a)] and μ_B [(b)] schemes, where the LQC model is presented by the black curve and the BDT models are presented by the blue, yellow and red curves, respectively for the choices, $(\phi, \dot{\phi}) = (1.5, 0)$, $(\phi, \dot{\phi}) = (1.0, 5.5 \times 10^{-5})$, and $(\phi, \dot{\phi}) = (1.0, -5.5 \times 10^{-5})$. The other initial conditions are the same as those given in Fig. 1 for the μ_A scheme, and those given in Fig. 2 for the μ_B scheme.

was previously seen in the LQC case [30, 47].

Finally, we note that we have explicitly verified that the values of the parameters and initial conditions chosen are quite generic in the sense that, by changing them to other reasonable values, we obtain similar behaviors, so our main conclusions and results are robust with different initial conditions. Also, in this section we do not include plots for the cases in which the massless scalar field Φ (which is equivalent to a stiff fluid) is present, as we find that it does not change the general results presented here, and the qualitative behavior also remains the same.

VI. CONCLUSIONS

In this paper we have derived the quantum-corrected effective background dynamics for BDT in the Bianchi I model in the Jordan's frame in the framework of LQG.

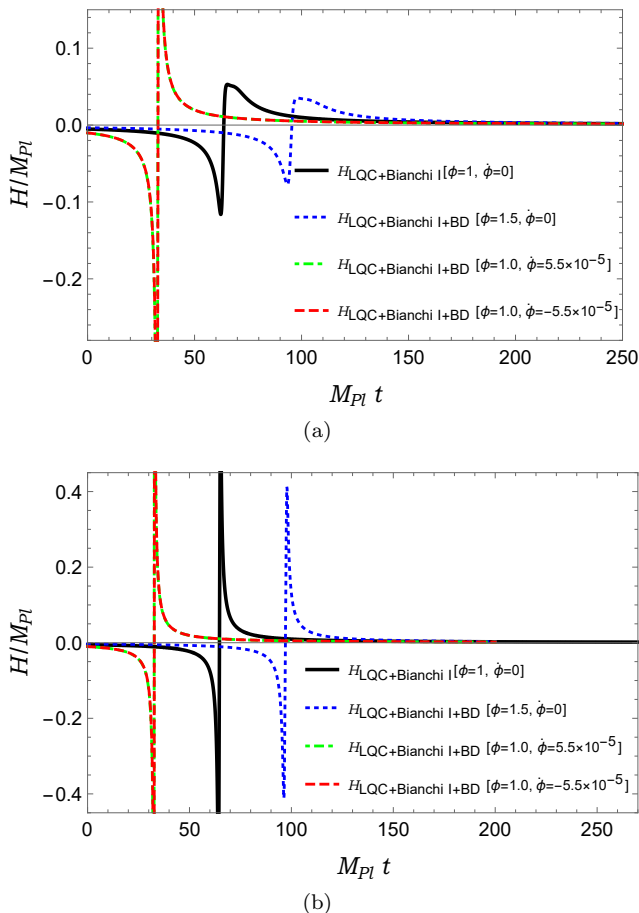


FIG. 4. The average Hubble parameters H of the Bianchi I spacetime for the $\bar{\mu}_A$ scheme [(a)] and the $\bar{\mu}_B$ scheme [(b)], where the LQC model is presented by the black curve and the BDT models are presented by the blue, yellow and red curves, respectively, for the choices, $(\phi, \dot{\phi}) = (1.5, 0)$, $(\phi, \dot{\phi}) = (1.0, 5.5 \times 10^{-5})$, and $(\phi, \dot{\phi}) = (1.0, -5.5 \times 10^{-5})$. The other initial conditions are the same as those given in Fig. 1 for the μ_A scheme and Fig. 2 for the μ_B scheme.

We have cast the theory in terms of the Yang-Mills phase space variables suitable for loop quantization and we have presented the quantum-corrected effective dynamics that resolve the spacetime singularity. The quantization is made by considering two different schemes, as given by Eqs. (4.2) and (4.18), respectively. The former set provides lower bounds on the scale factor, Eq. (4.17), proving the existence of a nonsingular quantum behavior of spacetime. On the other hand, the latter scheme gives us an upper bound to the effective energy density, i.e., the critical density ρ_c , implying a minimal value of spatial volume. Additionally, we have also derived the quantum corrected Friedmann equation for this model inspired by the idea of a directional energy density. We have explicitly shown that the effective dynamics of the Bianchi I Universe must undergo a smooth transition from a contracting phase to an expanding phase through the quantum bounce. Our analytical results, therefore, show

robustness of the singularity resolution and the consistency of the effective dynamics beyond general relativity.

In addition, we have also found different results obtained in BDT from those obtained in LQC. In particular, we have found that all the three directional scale factors are generically increasing after the quantum bounce and soon reach to their initial values, as can be seen from Figs. 1(c) and 1(d) for the μ_A scheme and in Figs. 2(c) and 2(d) for the μ_B scheme. This is sharply in contrast to the LQC case, in which one of the three directional scale factors is always decreasing after the bounce, and only two of them are increasing, as can be seen from Figs. 1(a) and 2(a) in both schemes.

As a perspective of future study in the context of the model considered here, it would be of interest to explore any possible observational features it might lead and that can be detected in the forthcoming cosmic microwave background experiments. An extension of the analysis, like the one performed in earlier studies in the context of LQC for homogeneous and isotropic models [75–79], would be of great interest.

Likewise, the analysis of the perturbations in the model presented here and the possibility of an inflationary phase following the quantum bounce could be eventually done. Concerning any possible observational signatures in LQC scenarios with an anisotropic background, one can mention, for instance, the work of Ref. [51], where an analysis of the possible observational features in such models was performed. Hence, an extension of such analysis of perturbations in the context of the BDT anisotropic LQC will be necessary in order to elaborate the observable predictions of the model.

Issues related to particle production due to the bounce can also be important [80–88] and their analysis and consequences in the context of anisotropic loop quantum BDT would be worthwhile to be pursued in the future as well.

ACKNOWLEDGMENTS

This work was partly done when M.S. was visiting the Inter-University Centre for Astronomy and Astrophysics (IUCAA), Pune, India. M.S. would like to express his sincere gratitude to Professor Dr. Naresh Dadhich for his kind invitation to visit IUCAA in the fall of 2022. The vibrant research environment and the scenic beauty of the campus was an impetus to carry this piece of work. L.L.G. is supported by research grants from Conselho Nacional de Desenvolvimento Científico e Tecnológico (CNPq), Grant No. 307636/2023-2 and from the Fundação Carlos Chagas Filho de Amparo à Pesquisa do Estado do Rio de Janeiro (FAPERJ), Grant No. E-26/201.297/2021. L.L.G. would like to thank IPMU–Kavli Institute for the Physics and Mathematics of the Universe for warm hospitality and also thank Professor Elisa Ferreira for the constant scientific inspiring discussions. R.O.R. acknowledges financial support by research grants from

Conselho Nacional de Desenvolvimento Científico e Tecnológico (CNPq), Grant No. 307286/2021-5, and from Fundação Carlos Chagas Filho de Amparo à Pesquisa

do Estado do Rio de Janeiro (FAPERJ), Grant No. E-26/201.150/2021. A.W. is partially supported by the US NSF Grant No. PHY2308845.

-
- [1] A. Ashtekar and E. Bianchi, A short review of loop quantum gravity, *Rep. Prog. Phys.* 84, 042001 (2021).
- [2] T. Thiemann, *Modern Canonical Quantum General Relativity* (Cambridge University Press, Cambridge, England, 2007), ISBN 978-0-511-75568-2, 978-0-521-84263-1, 10.1017/CBO9780511755682.
- [3] C. Rovelli, Loop quantum gravity, *Living Rev. Relativity* 11, 5 (2008).
- [4] M. Bojowald, *Canonical Gravity and Applications Cosmology, Black Holes, and Quantum Gravity* (Cambridge University Press, Cambridge, England, 2010), ISBN 978-0-521-19575-1, 978-0-511-98513-3.
- [5] R. Gambini and J. Pullin, *A First Course in Loop Quantum Gravity* (Oxford University Press, Oxford, 2011).
- [6] C. Rovelli and F. Vidotto, *Covariant Loop Quantum Gravity: An Elementary Introduction to Quantum Gravity and Spinfoam Theory* (Cambridge University Press, Cambridge, England, 2014), ISBN 978-1-107-06962-6, 978-1-316-14729-0.
- [7] T. Thiemann, Lectures on loop quantum gravity, *Lect. Notes Phys.* 631, 41 (2003).
- [8] A. Ashtekar and J. Lewandowski, Background independent quantum gravity: A status report, *Classical Quantum Gravity* 21, R53 (2004).
- [9] C. Rovelli, *Quantum Gravity* (University Press, New York, 2004), 10.1017/CBO9780511755804.
- [10] A. Ashtekar and J. Lewandowski, Differential geometry on the space of connections via graphs and projective limits, *J. Geom. Phys.* 17, 191 (1995)
- [11] A. Ashtekar and J. Lewandowski, Quantum theory of geometry II. Volume operators, *Adv. Theor. Math. Phys.* 1, 388 (1998).
- [12] A. Ashtekar and P. Singh, Loop quantum cosmology: A status report, *Classical Quantum Gravity* 28, 213001 (2011).
- [13] B. F. Li, P. Singh, and A. Wang, Phenomenological implications of modified loop cosmologies: An overview, *Front. Astron. Space Sci.* 8, 701417 (2021).
- [14] G. Barca, E. Giovannetti, and G. Montani, An overview on the nature of the bounce in LQC and PQM, *Universe* 7, 327 (2021).
- [15] B. F. Li and P. Singh, Loop quantum cosmology: Physics of singularity resolution and its implications, *arXiv:2304.05426*.
- [16] I. Agullo, A. Wang, and E. Wilson-Ewing, Loop quantum cosmology: Relation between theory and observations, *arXiv:2301.10215*.
- [17] E. Bianchi, The length operator in loop quantum gravity, *Nucl. Phys. B* 807, 591 (2009).
- [18] Y. Ma, C. Soo, and J. Yang, New length operator for loop quantum gravity, *Phys. Rev. D* 81, 124026 (2010).
- [19] M. Bojowald, Loop quantum cosmology, *Living Rev. Relativity* 8, 11 (2005).
- [20] R. H. Brandenberger, The matter bounce alternative to inflationary cosmology, *arXiv:1206.4196*.
- [21] J. L. Lehnert, Ekpyrotic and cyclic cosmology, *Phys. Rep.* 465, 223 (2008).
- [22] Y. F. Cai, R. Brandenberger, and P. Peter, Anisotropy in a nonsingular bounce, *Classical Quantum Gravity* 30, 075019 (2013).
- [23] M. Sharma, M. Shahalam, Q. Wu, and A. Wang, Preinflationary dynamics in loop quantum cosmology: Monodromy potential, *J. Cosmol. Astropart. Phys.* 11 (2018) 003.
- [24] W. J. Jin, Y. Ma, and T. Zhu, Pre-inflationary dynamics of Starobinsky inflation and its generalization in loop quantum Brans-Dicke cosmology, *J. Cosmol. Astropart. Phys.* 02 (2019) 010.
- [25] B. F. Li, P. Singh, and A. Wang, Qualitative dynamics and inflationary attractors in loop cosmology, *Phys. Rev. D* 98, 066016 (2018).
- [26] G. L. L. W. Levy and R. O. Ramos, α -attractor potentials in loop quantum cosmology, *Phys. Rev. D* 110, 043507 (2024).
- [27] M. Shahalam, M. Sharma, Q. Wu, and A. Wang, Preinflationary dynamics in loop quantum cosmology: Power-law potentials, *Phys. Rev. D* 96, 123533 (2017).
- [28] D. W. Chiou, Loop quantum cosmology in Bianchi type I models: Analytical investigation, *Phys. Rev. D* 75, 024029 (2007).
- [29] D. W. Chiou and K. Vandersloot, The Behavior of nonlinear anisotropies in bouncing Bianchi I models of loop quantum cosmology, *Phys. Rev. D* 76, 084015 (2007).
- [30] D. W. Chiou, Effective dynamics, big bounces and scaling symmetry in Bianchi type I loop quantum cosmology, *Phys. Rev. D* 76, 124037 (2007).
- [31] M. Martin-Benito, G. A. Mena Marugan, and T. Pawłowski, Loop quantization of vacuum Bianchi I cosmology, *Phys. Rev. D* 78, 064008 (2008).
- [32] A. Ashtekar and E. Wilson-Ewing, Loop quantum cosmology of Bianchi I models, *Phys. Rev. D* 79, 083535 (2009).
- [33] M. Martin-Benito, G. A. M. Marugan, and T. Pawłowski, Physical evolution in loop quantum cosmology: The example of vacuum Bianchi I, *Phys. Rev. D* 80, 084038 (2009).
- [34] A. Ashtekar and E. Wilson-Ewing, Loop quantum cosmology of Bianchi type II models, *Phys. Rev. D* 80, 123532 (2009).
- [35] A. Corichi and P. Singh, A geometric perspective on singularity resolution and uniqueness in loop quantum cosmology, *Phys. Rev. D* 80, 044024 (2009).
- [36] L. J. Garay, M. Martin-Benito, and G. A. Mena Marugan, Inhomogeneous loop quantum cosmology: Hybrid quantization of the Gowdy model, *Phys. Rev. D* 82, 044048 (2010).
- [37] E. Wilson-Ewing, Loop quantum cosmology of Bianchi type IX models, *Phys. Rev. D* 82, 043508 (2010).
- [38] B. Gupt and P. Singh, Contrasting features of anisotropic loop quantum cosmologies: The role of spatial curvature, *Phys. Rev. D* 85, 044011 (2012).
- [39] P. Singh and E. Wilson-Ewing, Quantization ambigu-

- ities and bounds on geometric scalars in anisotropic loop quantum cosmology, *Classical Quantum Gravity* 31, 035010 (2014).
- [40] P. Tarrao, M. F. Mendez, and G. A. M. Marugn, Singularity avoidance in the hybrid quantization of the Gowdy model, *Phys. Rev. D* 88, 084050 (2013).
- [41] L. Linsefors and A. Barrau, Exhaustive investigation of the duration of inflation in effective anisotropic loop quantum cosmology, *Classical Quantum Gravity* 32, 035010 (2015).
- [42] A. Corichi and E. Montoya, Loop quantum cosmology of Bianchi IX: Effective dynamics, *Classical Quantum Gravity* 34, 054001 (2017).
- [43] E. Wilson-Ewing, The loop quantum cosmology bounce as a Kasner transition, *Classical Quantum Gravity* 35, 065005 (2018).
- [44] I. Agullo, J. Olmedo, and V. Sreenath, Hamiltonian theory of classical and quantum gauge invariant perturbations in Bianchi I spacetimes, *Phys. Rev. D* 101, 123531 (2020).
- [45] I. Agullo, J. Olmedo, and V. Sreenath, Observational consequences of Bianchi I spacetimes in loop quantum cosmology, *Phys. Rev. D* 102, 043523 (2020).
- [46] A. M. McNamara, S. Saini, and P. Singh, Novel relationship between shear and energy density at the bounce in nonsingular Bianchi I spacetimes, *Phys. Rev. D* 107, 026003 (2023).
- [47] M. Motaharfar, P. Singh, and E. Thareja, Classicality and uniqueness in the loop quantization of Bianchi I spacetimes, *Phys. Rev. D* 109, 086013 (2024).
- [48] V. A. Belinsky, I. M. Khalatnikov, and E. M. Lifshitz, Oscillatory approach to a singular point in the relativistic cosmology, *Adv. Phys.* 19, 525 (1970).
- [49] P. K. Aluri, P. Cea, P. Chingangbam, M. C. Chu, R. G. Clowes, D. Hutsemekers, J. P. Kochappan, A. M. Lopez, L. Liu, N. C. M. Martens et al., Is the observable Universe consistent with the cosmological principle?, *Classical Quantum Gravity* 40, 094001 (2023).
- [50] S. Yeung and M. C. Chu, Directional variations of cosmological parameters from the Planck CMB data, *Phys. Rev. D* 105, 083508 (2022).
- [51] I. Agullo, J. Olmedo, and E. Wilson-Ewing, Observational constraints on anisotropies for bouncing alternatives to inflation, *J. Cosmol. Astropart. Phys.* 10 (2022) 045.
- [52] H. Amirhashchi, Probing dark energy in the scope of a Bianchi type I spacetime, *Phys. Rev. D* 97, 063515 (2018).
- [53] X. Zhang and Y. Ma, Nonperturbative loop quantization of scalar-tensor theories of gravity, *Phys. Rev. D* 84, 104045 (2011).
- [54] M. Artymowski, Y. Ma, and X. Zhang, Comparison between Jordan and Einstein frames of Brans-Dicke gravity a la loop quantum cosmology, *Phys. Rev. D* 88, 104010 (2013).
- [55] Y. Han, K. Giesel, and Y. Ma, Manifestly gauge invariant perturbations of scalar-tensor theories of gravity, *Classical Quantum Gravity* 32, 135006 (2015).
- [56] Y. Han, Loop quantum cosmological dynamics of scalar tensor theory in the Jordan frame, *Phys. Rev. D* 100, 123541 (2019).
- [57] S. Song, C. Zhang, and Y. Ma, Alternative dynamics in loop quantum Brans-Dicke cosmology, *Phys. Rev. D* 102, 024024 (2020).
- [58] X. Zhang, J. Yu, T. Liu, W. Zhao, and A. Wang, Testing Brans-Dicke gravity using the Einstein telescope, *Phys. Rev. D* 95, 124008 (2017).
- [59] C. Kiefer, *Quantum Gravity*, 3rd ed. (Oxford University Press, England, 2012).
- [60] B. S. DeWitt and G. Esposito, An introduction to quantum gravity, *Int. J. Geom. Methods Mod. Phys.* 05, 101 (2008).
- [61] J. C. Baez and J. P. Muniain, *Gauge Fields, Knots and Gravity* (World Scientific Publishing Company, Singapore, 1994), Vol. 4.
- [62] G. J. Olmo and H. Sanchis-Alepuz, Hamiltonian formulation of Palatini $f(R)$ theories a la Brans-Dicke, *Phys. Rev. D* 83, 104036 (2011).
- [63] R. T. Jantzen, Spatially homogeneous dynamics: A unified picture, arXiv:gr-qc/0102035.
- [64] V. Taveras, Corrections to the Friedmann equations from LQG for a Universe with a free scalar field, *Phys. Rev. D* 78, 064072 (2008).
- [65] P. Singh, Are loop quantum cosmos never singular?, *Classical Quantum Gravity* 26, 125005 (2009).
- [66] W. Kaminski, M. Kolanowski, and J. Lewandowski, Dressed metric predictions revisited, *Classical Quantum Gravity* 37, 095001 (2020).
- [67] A. Corichi, T. Vukasinac, and J. A. Zapata, Polymer quantum mechanics and its continuum limit, *Phys. Rev. D* 76, 044016 (2007).
- [68] E. Giovannetti, G. Barca, F. Mandini, and G. Montani, Polymer dynamics of isotropic universe in ashtekar and in volume variables, *Universe* 8, 302 (2022).
- [69] W. C. Gan, X. M. Kuang, Z. H. Yang, Y. Gong, A. Wang, and B. Wang, Nonexistence of quantum black and white hole horizons in an improved dynamic approach, *Sci. China Phys. Mech. Astron.* 67, 280411 (2024).
- [70] W.-C. Gan and A. Wang, A new quantization scheme of black holes in effective loop quantum gravity, *Phys. Rev. D* 111, 026017 (2025).
- [71] A. Ashtekar, M. Bojowald, and J. Lewandowski, Mathematical structure of loop quantum cosmology, *Adv. Theor. Math. Phys.* 7, 233 (2003).
- [72] A. Ashtekar, T. Pawlowski, and P. Singh, Quantum nature of the big bang: An analytical and numerical investigation, *Phys. Rev. D* 73, 124038 (2006).
- [73] A. Ashtekar, T. Pawlowski, and P. Singh, Quantum nature of the big bang: Improved dynamics, *Phys. Rev. D* 74, 084003 (2006).
- [74] X. Zhang, Loop quantum cosmology, modified gravity and extra dimensions, *Universe* 2, 15 (2016).
- [75] I. Agullo, A. Ashtekar, and W. Nelson, The preinflationary dynamics of loop quantum cosmology: Confronting quantum gravity with observations, *Classical Quantum Gravity* 30, 085014 (2013).
- [76] T. Zhu, A. Wang, G. Cleaver, K. Kirsten, and Q. Sheng, Pre-inflationary universe in loop quantum cosmology, *Phys. Rev. D* 96, 083520 (2017).
- [77] M. Benetti, L. Graef, and R. O. Ramos, Observational constraints on warm inflation in loop quantum cosmology, *J. Cosmol. Astropart. Phys.* 10 (2019) 066.
- [78] L. N. Barboza, G. L. L. W. Levy, L. L. Graef, and R. O. Ramos, Constraining the Barbero-Immirzi parameter from the duration of inflation in loop quantum cosmology, *Phys. Rev. D* 106, 103535 (2022).
- [79] L. N. Barboza, L. L. Graef, and R. O. Ramos, Warm

- bounce in loop quantum cosmology and the prediction for the duration of inflation, *Phys. Rev. D* 102, 103521 (2020).
- [80] L. L. Graef, R. O. Ramos, and G. S. Vicente, Gravitational particle production in loop quantum cosmology, *Phys. Rev. D* 102, 043518 (2020).
- [81] J. Quintin, Y. F. Cai, and R. H. Brandenberger, Matter creation in a nonsingular bouncing cosmology, *Phys. Rev. D* 90, 063507 (2014).
- [82] Y. Tavakoli and J. C. Fabris, Creation of particles in a cyclic universe driven by loop quantum cosmology, *Int. J. Mod. Phys. D* 24, 1550062 (2015).
- [83] J. Haro and E. Elizalde, Gravitational particle production in bouncing cosmologies, *J. Cosmol. Astropart. Phys.* 10 (2015) 028.
- [84] D. C. F. Celani, N. Pinto-Neto, and S. D. P. Viteni, Particle creation in bouncing cosmologies, *Phys. Rev. D* 95, 023523 (2017).
- [85] A. Scardua, L. F. Guimarães, N. Pinto-Neto, and G. S. Vicente, Fermion production in bouncing cosmologies, *Phys. Rev. D* 98, 083505 (2018).
- [86] W. S. Hipolito-Ricaldi, R. Brandenberger, E. G. M. Ferreira, and L. L. Graef, Particle production in ekpyrotic scenarios, *J. Cosmol. Astropart. Phys.* 11 (2016) 024.
- [87] L. L. Graef, W. S. Hipolito-Ricaldi, E. G. M. Ferreira and R. Brandenberger, Dynamics of cosmological perturbations and reheating in the anamorphic universe, *J. Cosmol. Astropart. Phys.* 04 (2017) 004.
- [88] G. S. Vicente, R. O. Ramos and L. L. Graef, Gravitational particle production and the validity of effective descriptions in loop quantum cosmology, *Phys. Rev. D* 106, 043518 (2022).